Engineering Geology 294 (2021) 106324

Contents lists available at ScienceDirect

Engineering Geology

journal homepage: www.elsevier.com/locate/enggeo

Combined portable free fall penetrometer and chirp sonar measurements of three texas river sections post hurricane harvey

Reem Jaber [a,*], Nina Stark [a], Navid Jafari [b], Nadarajah Ravichandran [c]

[a] Department of Civil and Environmental Engineering, Virginia Tech, 200 Patton Hall, Blacksburg, VA 24061, United States of America
[b] Department of Civil and Environmental Engineering, Louisiana State University, 3212D Patrick F. Taylor Hall, Baton Rouge, LA 70803, United States of America
[c] Department of Civil Engineering, Clemson University, 202 Lowry Hall, Clemson, SC 29634, United States of America

ARTICLE INFO

Keywords:
Portable free fall penetrometer
Chirp sonar
Site characterization
Fluvial sediment dynamics
Sediment strength

ABSTRACT

The US Gulf of Mexico coastal region has repeatedly been subjected to major flood events. Local geotechnical site characteristics and geomorphology can change due to sediment transport processes during such events. However, field measurements during extreme conditions are challenging. This paper discusses initial attempts at a combined geotechnical and geophysical site investigation of the uppermost layers of riverbeds following severe flooding events at three different rivers in Texas: the Guadalupe, Brazos, and Colorado Rivers in terms of sediment strength derived from a portable free fall penetrometer, backscatter intensity recorded by a chirp sonar, and soil sample characterization. Results show low strength sediments (<40 kPa) along the investigated sections of the Guadalupe and Brazos riverbanks. Although sediments in the center of the Brazos River were characterized with higher strength (>50 kPa) and larger grain sizes ($d_{50} \sim 0.3$ mm), sediment strength of the Guadalupe and Colorado Rivers displayed more variations around bridge piers. The spatial variations likely resulted from sediment remobilization processes and local scour under severe hydrodynamic conditions. Both, geotechnical and geophysical results, reflected the observed variations in the riverbed sediments; nonetheless, a quantitative correlation among the rivers was impeded by challenges primarily related to limitations of spatial accuracy and the significant riverbed heterogeneity, as well as shallow water limitations of the chirp sonar.

1. Introduction

Hurricanes have impacted the Gulf of Mexico over the last decades, including Hurricanes Harvey and Ike in Texas, which caused a significant number of fatalities and loss of property (Zane et al., 2011; Qin et al., 2020). Energetic hydrodynamics and flooding events during hurricanes can augment local sediment dynamics in coastal environments such as Texas rivers (Collins et al., 1979; Stone et al., 2004; Xu et al., 2016). Texas rivers are highly geomorphodynamic and particularly prone to meander migration, providing more motivation to investigate their sediment remobilization processes, especially those prone to extreme events (Briaud et al., 2002).

Sediment remobilization processes and riverbed geomorphodynamics are expected to affect geotechnical site characteristics (Stark and Kopf, 2011). Specifically, this may include the evolution and destruction of bedforms, such as ripples and bars, scour around subaqueous infrastructure, deepening or shoaling of river sections, and river meanders. This can add risk to infrastructure and present safety hazards in terms of compromising the stability of bridge pillars, destabilization of riverbanks, and undermining of electrical power transmission lines (Briaud et al., 1999). Thus, there is a need for assessment methods that will enable a rapid and safe geotechnical site investigation shortly after and possibly during severe sediment remobilization events in riverine environments.

Portable free fall penetrometers (PFFP) have emerged as a rapid in-situ investigation method to measure the topmost layers of the seabed and riverbed surfaces in areas of difficult access (Spooner et al., 2004; Randolph, 2016) and to investigate sediment transport processes from a geotechnical perspective (Stark and Kopf, 2011). While PFFP data analysis was initially limited to a rapid seabed classification (Stoll and Akal, 1999), researchers have continued to develop approaches towards a quantitative site characterization from PFFP. These approaches include estimating shear strength or bearing strength, friction angle, and relative density of surficial seabed sediments, as well as looking in more detail at seabed stratification and relationships between geotechnical parameters and local sediment dynamics (Akal and Stoll, 1995; Silva

* Corresponding author.
E-mail addresses: reemj@vt.edu (R. Jaber), ninas@vt.edu (N. Stark), njafari@lsu.edu (N. Jafari), nravic@clemson.edu (N. Ravichandran).

https://doi.org/10.1016/j.enggeo.2021.106324
Received 11 February 2021; Received in revised form 27 July 2021; Accepted 6 August 2021
Available online 11 August 2021

et al., 2006; Seifert et al., 2008; Stark and Kopf, 2011; Seifert and Kopf, 2012; Dorvinen et al., 2018; Albatal et al., 2019). Laboratory testing, including vane shear, triaxial, and direct shear, has been used to compare and validate PFFP results in terms of the estimated soil strength properties (Mosher et al., 2007; Seifert et al., 2008; Chow and Airey, 2013; Albatal et al., 2020).

In the early stages of PFFP development, a key motivation was the potential combined use with acoustic methods (Spooner et al., 2004). Acoustic methods provide a qualitative seabed sediment characterization and several attempts have been made to correlate the geoacoustic seabed properties with geotechnical sediment properties (Holland, 2002; Osler et al., 2002; Jackson and Richardson, 2007; Anderson et al., 2008; Harris et al., 2008; Brown et al., 2011; Long et al., 2020). Chirp sonars and other acoustic sub-bottom profilers are also often combined with cone penetration testing (CPT) and core sampling for an efficient offshore site investigation (Houlsby and Ruck, 1998; Saleh and Rabah, 2016). High resolution seismic tools have also been integrated with CPT to identify varying soil behavior types at shallow depths (Long et al., 2020; Prins and Andresen, 2021). PFFPs were envisioned as a rapid and cost-effective means to improve the calibration of acoustic methods with regards to seabed properties, such as undrained shear strength, porosity, and bulk density (Osler et al., 2006; Abelev et al., 2017). At the same time, acoustic surveying provides a larger and more efficient spatial coverage than penetrometers and physical testing methods (Mcneill, 1979; Schrottke et al., 2006; Abelev et al., 2017; Prins and Andresen, 2021). While the advantages of combined acoustic and seismic surveying and penetrometer seabed deployments are understood, limited examples of correlation efforts using PFFPs are available in the literature (Osler et al., 2002; Mayne, 2014; Long et al., 2020; Prins and Andresen, 2021). To the best of our knowledge, none has focused on post-flooding investigations in rivers.

Chirp sonars offer scanning of the seabed to sediment depths on the order of tens of meters while maintaining a resolution on the order of centimeters, providing insights into seabed stratification in terms of its acoustic impedance governed by soil type and soil packing among other factors (Neto et al., 2013). While they are commonly applied in offshore site investigation, chirp sonars are rarely deployed in shallow water bodies. More recent instrument developments offer the potential application in rivers (also with shallower water depths of only 1 to 5 m). Thus, it is hypothesized that chirp sonar can assist with detecting and quantifying freshly deposited and relocated sediment layers after flood events in rivers and that new insights into sediment remobilization, deposition, and possibly subsequent consolidation can be achieved through a combined use of PFFP and chirp sonar.

During Hurricane Harvey in 2017, a team mobilized by the NSF Geotechnical Extreme Events Reconnaissance association (GEER) identified severe erosion and sediment transport events along the Guadalupe, Colorado, and Brazos Rivers, Texas (Stark et al., 2017). Specific concerns included the deposition of large sediment volumes from riverbank failures, scour at subaqueous structures, and effects of river meandering. At the time of the reconnaissance mission (2 days after landfall), access to the rivers was limited due to the continuing flooding over riverbanks, high velocity flows, and debris carried by the rivers. During successive site investigations, conditions were expected to be affected by changes in hydrodynamic conditions and subsequent infill of potential scour holes and erosion hotspots (Gavin and Prendergast, 2018; Link et al., 2020).

This paper presents data from exploratory field surveys of sections of the Guadalupe, Brazos, and Colorado Rivers in Victoria, Sugarland, and Bay City, Texas. Each site is characterized by unique geomorphological conditions as well as differences regarding nearby local infrastructure. The field measurements were conducted in July 2018, about ten months after Hurricane Harvey made landfall. Field measurement techniques included chirp sonar, PFFP, and sediment grab sampling, among others that are out of the scope of this study. All measurements were performed from small vessels, such as canoes and a 2.5 m inflatable zodiac, due to still limited access to some river sections from damage to boat ramps at the Guadalupe and the Brazos Rivers. This article addresses the following main research questions: (1) Can chirp sonar measurements complement PFFP measurements for sediment characterization in a riverine environment? (2) Can combined in-situ geotechnical, geoacoustic, and laboratory tests (specifically testing of soil erodibility) reveal new information on local sediment remobilization processes? and (3) How do geotechnical sediment characteristics relate to local sediment dynamics and environmental conditions in three rivers affected by Hurricane Harvey?

2. Regional context

In August 2017, Hurricane Harvey developed as a category 4 hurricane on the Saffir-Simpson scale over the Gulf of Mexico, eventually causing flooding along three rivers investigated in this study: Guadalupe, Brazos, and Colorado Rivers (Fig. 1a). The following sections provide more details on the specific locations surveyed within each river.

2.1. Guadalupe River

The Guadalupe River stretches over a length of 380 km from Kerr County, Texas, to San Antonio Bay in the Gulf of Mexico. The survey site (28°45'06.89" N, 97°00'24.78" W) is in the lower reach in Victoria, Texas, and features significant river meanders (Fig. 1b). The USGS river gage 08176500 in Victoria, Texas, shows an average annual water flow of 55 m^3/s and an average annual stage of 2.77 m in 2017 (NWIS, 2019). On August 31, 2017, during the flooding from Hurricane Harvey, water levels reached 10.5 m (NWIS, 2019) as shown in Fig. S1 (provided in a companion Data in Brief article with more information). Field measurements included cross-river and along-river transects and measurements around the piles of the E Frontage Rd Bridge.

2.2. Brazos River

The Brazos River watershed stretches from New Mexico to the Gulf of Mexico. The study area (29°34'20.99" N, 95°41'51.81" W) is near the cities of Sugarland and Richmond (Fig. S2). Several locations near the Brazos River survey area suffered riverbank erosion and slope failures (Stark et al., 2017). Water levels and discharge rates recorded during Hurricane Harvey exceeded historical levels. Maximum water levels recorded by the USGS river gage 08114000 of the Brazos River at Richmond, Texas, reached ~16.8 m on August 31, 2017 (statistic daily mean ~ 7.6 m), which corresponded to a discharge over 2830 m^3/s (statistic daily mean ~ 43 m^3/s) (Stark et al., 2017; NWIS, 2019). According to a study by Blake and Zelinsky (2018), the Brazos River is considered highly susceptible to erosion during flood events. Riverbanks in the proximity of the study area eroded in some locations up to ~44 m during the last decade (Fig. S3).

2.3. Colorado River

Colorado River is the longest river in Texas (2330 km). The survey site (28°59' 02.41" N, 96°00'01.28" W) is shown in Fig. 2. Recorded water levels reached 14 m on September 2, 2017 and river discharge exceeded 140 m^3/s, compared to an annual average water level of 1.8 m and annual average water flow of 76.2 m^3/s according to the USGS gage 08162500 (NWIS, 2019). West of the Houston ship channel (near the survey site), sediments primarily consist of muddy sands, with sand content increasing near the mouth of the Colorado River (McGowen et al., 1979).

3. Methods

A number of geotechnical and geophysical devices were deployed

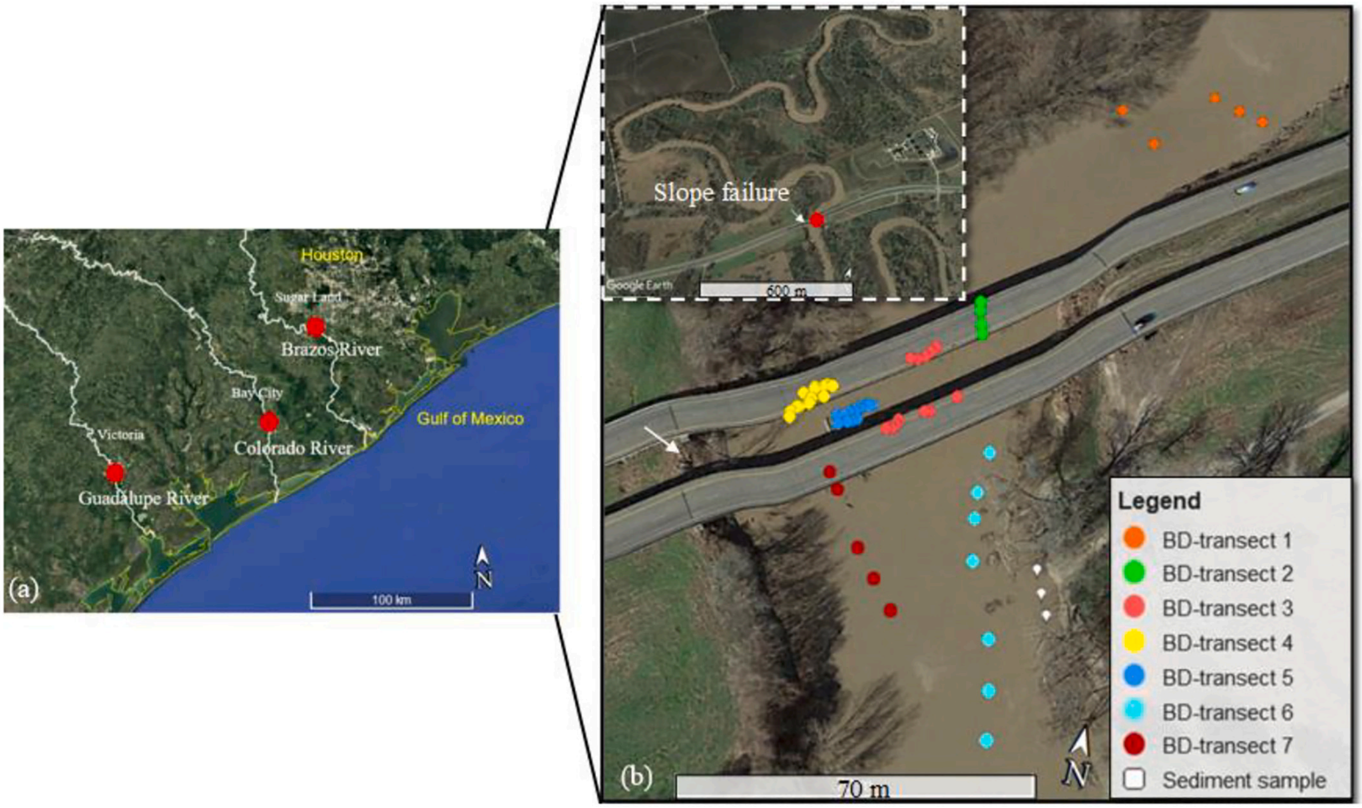

Fig. 1. Google Earth (2018) image of the (a) survey locations in the Guadalupe, Brazos, and Colorado Rivers in Texas, (b) PFFP deployments and sediment sampling locations at Guadalupe River, Texas (28°45′06.89" N, 97°00′24.78" W) (Map data: Google, SIO, NOAA, US Navy, NGA, GEBCO).

during the survey. However, this article will focus on the PFFP and chirp sonar results as well as complementary sediment sampling.

3.1. Portable Free Fall Penetrometer (PFFP)

The PFFP *Bluedrop* used in this study has a streamlined shape and can be deployed "freely" by hand from small vessels. The PFFP records decelerations at a sampling rate of 2 kHz, using five vertical micro-electromechanical systems (MEMS) accelerometers and measures hydrostatic and pore pressure up to 2 MPa through a pressure transducer located ~8 cm behind the cone. The advancement of the PFFP through the soil depends mainly on the soil resistance that eventually forces the penetrometer to a halt. The other resisting forces (soil buoyancy and drag) are neglected due to the shallow penetration depth. The measured deceleration during riverbed penetration can be correlated to an equivalent of soil bearing capacity using the procedure explained by Stark et al. (2011), and therefore, will be briefly mentioned here. The force decelerating the PFFP is calculated based on the deceleration profiles using Newton's second law. The force is then divided by the area subjected to the load to get the dynamic bearing capacity. However, the penetration rate of the PFFP is considered high compared to the constant penetration rate of the CPT (2 cm/s) and required correction by a strain rate factor to obtain the quasi-static bearing capacity (*qsbc*) (Dayal and Allen, 1973; Stark et al., 2011). The first and second derivatives of the deceleration-time profile represent the probe's velocity and the penetration depth, respectively.

For the analysis of the pore-water pressure (PWP), only measurements with a full embedment of the pressure sensor (7.57 cm from the tip) were considered. Deployments with penetration depth less than 15 cm (55%) were excluded from the analysis. Additional deployments (10%) were omitted due to a delayed response likely from lack of saturation in the pressure filter ring. Sandven (2010) and Seifert et al. (2008) describe the potential difficulty and importance of full saturation of the filter ring and pore water inlets connecting the pressure transducer with the surrounding environment for subaerial cone and submarine free fall penetrometers, respectively. In this study, the heat and limited on-vessel infrastructure and space, e.g., that enables submerged storage between deployments, represented additional challenges regarding maintaining full saturation of the filter ring and pore water inlets.

3.2. Chirp Sonar

The *SyQwest Stratabox HD* chirp sonar system is a portable, high-resolution acoustic instrument that can resolve seabed strata to sediment depths of ~40 m, with a vertical resolution of up to 6 cm. It is suitable for water depths ranging from <2.5 m (bottom type dependent) to 150 m. The transmit rate is up to 10 Hz and the frequency is 10 kHz (SyQwest, 2016). The chirp sonar detects the reflection of the transmitted sound pulses from different soil layers with different geoacoustic properties. The distance traveled by the reflected signal and the time needed to reach the source/receiver is used to determine the depth of the soil layer, while the backscatter intensity (i.e., the strength of the return signal) can reflect different geoacoustic properties and thus the soil type (Harris et al., 2008). In this study, signal post-processing is limited to the depicting of different riverbed layers according to the amplitude envelope of the reflected signal using the manufacturer's software (Wang and Stewart, 2015). Generally, high backscatter intensity indicates strong reflection off the soil layer, while low backscatter intensity suggests that the majority of the acoustic pulse is propagating through the soil layer. This is governed by soil properties, such as bulk density and porosity, shear strength, clay/silt/sand content, and other geotechnical properties (Jackson and Richardson, 2007). Preston et al. (1999) found that strength-related properties correlate better with low (i.e., 38 kHz)

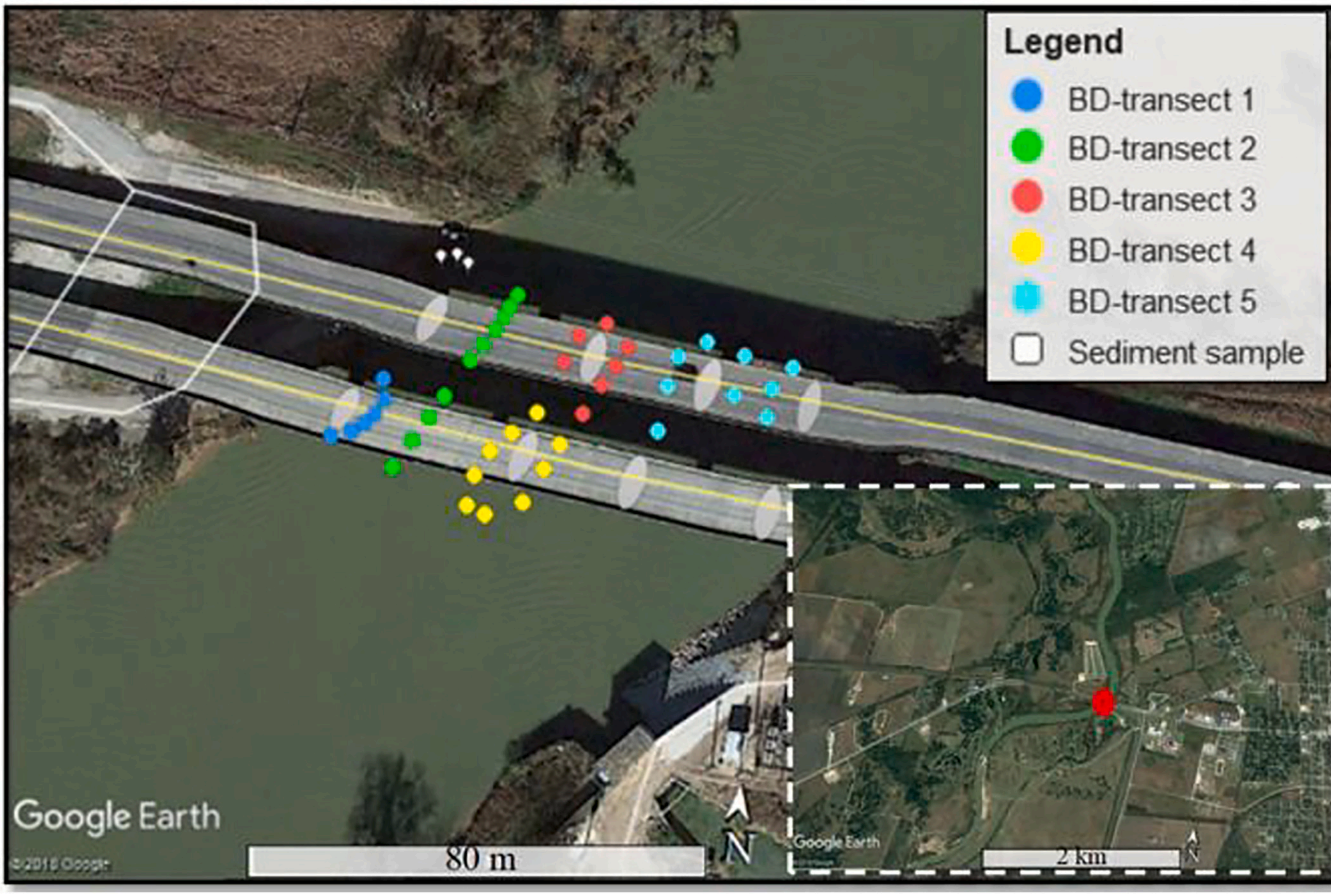

Fig. 2. Google Earth (2018) image of the Colorado River, Texas 28°59'02.41" N, 96°00'01.28" W. PFFP deployments and sediment sampling locations are highlighted. The oval grey objects represent the 8 pillars of the bridge (Map data: Google, SIO, NOAA, US Navy, NGA, GEBCO).

frequencies. However, surface properties as grain size and porosity seem to correlate better with high frequencies (i.e., 200 kHz). Harris et al. (2008) describe different techniques to estimate geotechnical properties from geoacoustic properties, such as impedance and acoustic texture. Although geoacoustic properties can be related more directly to geotechnical properties, there is still a number of open questions that hamper a straightforward correlation in field studies. Also, shallow water conditions and vessel limitations may affect geoacoustic data quality in a way that may limit the direct derivation of geotechnical properties from acoustic surveying. Here, it is attempted to correlate the relatively low frequency (10 kHz) geoacoustic data to PFFP data towards pathways of combined use of PFFP and sub-bottom acoustic profilers in riverine post-flood event surveying. Chirp sonar transects were performed in all three rivers as much in line with the PFFP deployments as conditions allowed. For navigational reasons of the small vessels, uncertainty in position on the order of meters cannot be excluded.

3.3. Acoustic Doppler Current Profiler (ADCP)

An acoustic Doppler current profiler (ADCP), *Nortek AquaDopp HR*, was used to measure the water flow velocity at the Guadalupe and Colorado Rivers during the collection of the geotechnical data. These measurements did not succeed in the Brazos River due to timing issues. The instrument was mounted on the top of a platform and lowered to the riverbed close to the PFFP deployments, at the eastern riverbank downstream the bridge (28°45' 5.74" N, 97°00'24.28" W) and at the western riverbank upstream the bridge (28°59'03.07" N, -96°00'01.37"W) at Guadalupe and Colorado Rivers, respectively. The device measures flow velocities along an 80 cm-long vertical profile with a 3 cm resolution and a blanking distance of 9.6 cm above the AquaDopp HR. The velocity profiles were averaged over the measurement period.

3.4. Sediment sampling and laboratory testing

A petite (7 kg) ponar sediment grab sampler (EcoEnvironmental, 2019) and a push tube sampler were used to collect sediments from the riverbed for grain size analysis. Three samples were collected from the Guadalupe and Colorado Rivers, respectively (Figs. 1 and 2). Samples from the Brazos River site were collected at seven locations across the river and along the riverbanks (Fig. S2). Due to the mostly non-cohesive nature of the soils and the sampling methods, the samples were considered disturbed. Grain size analysis was performed on each of the samples per ASTM D6913.

The erosion function apparatus (EFA) measured the erodibility of soil under shear stresses exhibited by flow at controlled velocities (Briaud et al., 2001). A sediment tube of the collected soil sample was introduced at the bottom of the conduit in which water flowed at a certain speed (Shidlovskaya et al., 2016). If the shear stress applied by the flow on the soil sample surface exceeded the critical shear stress, erosion is initiated, and the erosion volume can be measured over time for given shear stresses. The results are presented as erosion rate per flow velocity and classified into five groups of erodibility based on the erosion volume. EFA tests were performed on four (4) samples from the Guadalupe, five (5) from the Brazos, and seven (7) from the Colorado River under velocities ranging from 0.2 m/s to 5.6 m/s (observed at Brazos River).

4. Results

The results are organized by river investigated. It should be noted that some of PFFP deployments were removed from the analysis due to apparent impacts with debris or pillar edges.

4.1. Guadalupe River

Twenty-seven PFFP deployments were carried out at different locations in the vicinity of the Frontage Rd Bridge over the Guadalupe River near Victoria, Texas, on July 16–17 (see Fig. 1). Based on their locations, the deployments were grouped and divided into six transects in Fig. 3 displaying the maximum *qsbc* recorded. The detailed *qsbc* profiles with depth are presented in Fig. 3, where profile colors reflect the different *qsbc* groups (Fig. S4) merged into three groups: 0–40 kPa, 40–100 kPa, and 100–150 kPa.

The impact velocity of the PFFP ranged from 3.8 to 5.8 m/s, with an average of 5 m/s, and a standard deviation of 0.4 m/s. Two out of five deployments along transect 1 (upstream of the bridge) were characterized by a distinct profile showing a steady increase of *qsbc* between a sediment depth of 5–23 cm, yielding a maximum *qsbc* of ~10 kPa. The other profiles suggested stiffer sediments reaching a maximum *qsbc* ~50 kPa at a sediment depth of only 5–10 cm. Transect 2 located near one of the piles of the bridge towards the center of the river was characterized by softer sediments with *qsbc* ~ 12–22 kPa in the upper ~20 cm of the river bed. Transect 3, near the most downstream pile of the bridge and towards the center of the river, exhibited hard sediments reaching up to 100 kPa at sediment depths <15 cm. Most of the deployments along transect 4, between the western shore and a bridge pile, were omitted from the study results due to impacts with debris. The only *qsbc* profile seems to slowly increase to a maximum *qsbc* of ~50 kPa at a depth of 14 cm. The majority of transect 5 deployments, just south of transect 4, were characterized by relatively soft sediments. Deployments among transect 6, downstream of the bridge and near the eastern shore, were the most consistent and can be represented by a steady increase in the *qsbc* to a maximum of ~25 kPa at a depth of 10–15 cm below the riverbed. The topmost 5 cm of the riverbed appears to be looser sediments with the potential presence of benthic biogenic processes, some vegetation, and/or small debris (e.g., sticks). Assuming that transect 6 represents typical sediment strength profiles of this section of the Guadalupe River away from infrastructure and meandering suggests that the presence of the bridge within the meander section leads to surficial riverbed softening or hardening in a complex manner with few clear trends being visible.

The PWP responses varied among the three rivers, but all responses were grouped and divided based on three distinctive types: Type A, B, and C (Fig. S5). Type A profiles were characterized by sub-hydrostatic pressures (i.e., deviates from the projection of hydrostatic increase with depth by smaller values) developing just before and during penetration, and none to a slight increase in pore pressure with time during rest within the river bed. The continuous sub-hydrostatic (below hydrostatic pressure) response with further penetration has been observed earlier and correlated to dilative silty sands (Lucking et al., 2017). This agrees with the fine sand (average d_{50} of 0.15 mm) classification observed at this location with 25% fines. The recorded pressure records of Type B deviated from the hydrostatic projection towards sub-hydrostatic pressures during penetration and changed towards supra-hydrostatic pressures (higher pressure than the projected hydrostatic pore pressure) upon rest in the riverbed. Type B response in sediments has been previously associated with mixed soils, including clayey and sandy soils (Lucking et al., 2017). No samples were retrieved at this deployment location to confirm the sediment type. However, similar behavior was observed at locations classified as medium sand (<3% fines) with an average d_{50} of 0.59 mm. Almost all sediments at the Guadalupe River exhibited a Type B PWP response, except for transect 1 upstream profiles which showed variations between Types A and B. Although the percent fines did not exceed 15% at the riverbanks, it may have increased in the river center and around bridge piers. Type C pore pressure responses were characterized by a pore pressure response identical to the projected hydrostatic pressure and supra-hydrostatic (above hydrostatic pressure) during penetration with little change of the penetrometer at rest. This behavior was not observed in the Guadalupe River.

An example of the output of the chirp sonar in terms of the normalized chirp backscatter intensity (*NBI*) in the upper meter of the riverbed in the vicinity of transect T2 (Fig. 1) is shown in Fig. 4. Locations G1 and G2 (water depths ~3 m) are characterized by a lesser increase in *NBI* with depth, reaching *NBI* >90% at a sediment depth of ~20 cm. At G3, *NBI* >90% is achieved at a sediment depth of ~15 cm, and at G4 and G5 *NBI* yielded only ~50% in the investigated top 30 cm. Lower *NBI* may be associated with less dense or less strong sediments, as well as with more a more complex roughness leading to more loss of signal due to scattering.

Fig. 5 compares the PFFP and the chirp sonar measurements of (a) water depth and (b) soil properties in terms of *qsbc* and *NBI* at the measurement locations shown in Fig. 5(c). The instruments were not deployed concurrently, leading to spatial uncertainties regarding the measurement locations in the order of meters between the two instruments. The water depths determined by the chirp sonar were almost identical to the water depths estimated by the PFFP (Fig. 5a). Some variations were recorded at location GD, which can be attributed to the spatial variability of the deployment locations between the chirp and the PFFP. The match between both results highlights the importance of the simplified Bernoulli correction adapted to correct the water depths measured by the PFFP (Mumtaz et al., 2018). Fig. 5(b) shows a comparison between the *qsbc* and *NBI* values measured 5–7 cm and 10–12 cm below the riverbed. The best expected vertical resolution of the chirp sonar is 6 cm, which means that the shallower measuring point may be affected by varying contributions of seabed and water column with small-scale changes in seabed topography. At the shallower penetration depth, an opposing trend could be observed showing an increase in *NBI* with a decrease in strength. This trend appears counterintuitive. However, this may be related to the effects of changing surface roughness (i.e., small-scale topography) which may also relate to changes in grain size. No trend appeared visible at the slightly deeper penetration depth.

Based on the unified soil classification system ((ASTM D2487–11, 2021)), the samples collected in the Guadalupe River classified as fine to medium poorly graded sands (SP), with median grain size (d_{50}) between 0.19 and 0.59 mm and fines content between 3% and 12% (ASTM D6913–17, 2021) (Fig. 6a). Only limited sediment samples were collected from the site (close to riverbanks), and thus, the results may not be representative of all locations tested. No detailed information on the surficial sediment properties could be identified in the literature, limiting further comparison with the current results.

The average flow speed over this measurement duration and the measured profile (up to 1 m above the riverbed) was 0.21 m/s. For a better understanding of the sediment dynamics associated with the measured river flow velocity, the flow velocity is compared with the threshold needed to initiate sediment motion or erosion, often represented as Shields parameter. Critical velocity (V_c) or critical shear stress represents the erosion threshold needed for erosion to initiate. The critical velocity (Eq. 1) is based on the model suggested. by Briaud (2013) and EFA results (Fig. 6b). This model predicts the critical velocity needed for sediment erosion based on the mean grain size for sand sediment with d_{50} between 0.1 and 10 mm, which agrees with the sediment type and grain size observed here. It was developed based on EFA measurements and incorporated the data used by Shields (1936), making it more relevant to the data presented here.

$$V_c = 0.35(d_{50})^{0.45} \tag{1}$$

The critical velocity estimated from Briaud's model is 0.22 m/s based

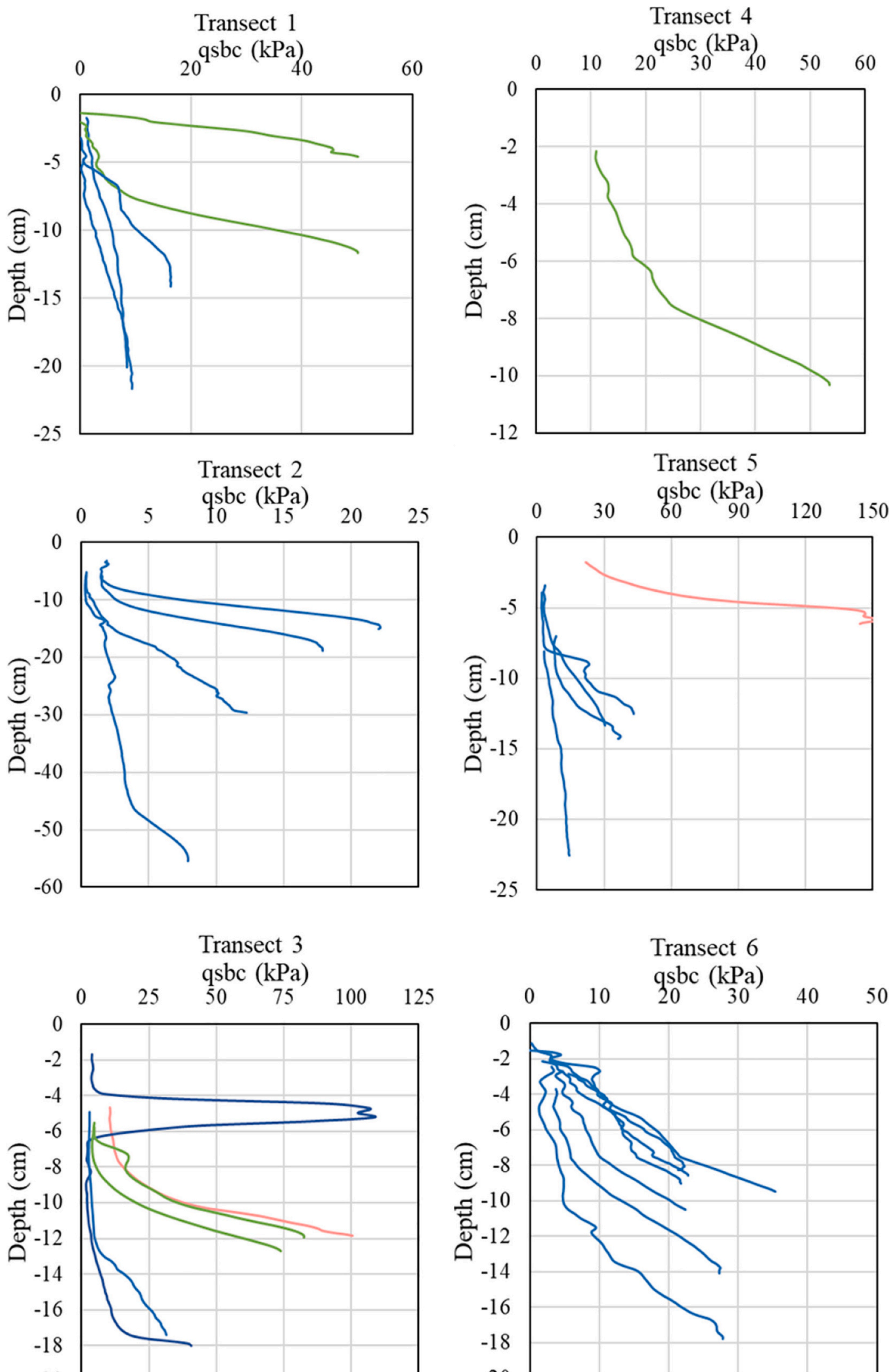

Fig. 3. Quasi-static bearing capacity *(qsbc)* profiles at each transect at Guadalupe River. The three colors represent the maximum *qsbc*: blue color 0–40 kPa, green color 40–100 kPa, pink color 100–150 kPa. (For interpretation of the references to color in this figure legend, the reader is referred to the web version of this article.)

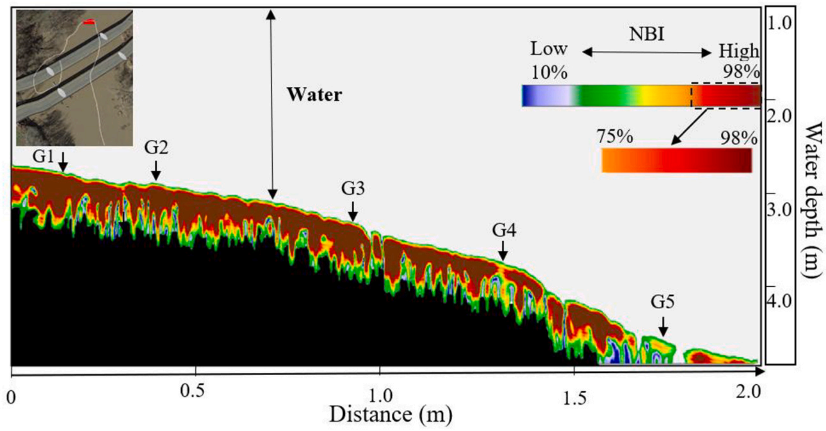

Fig. 4. Chirp sonar normalized backscatter intensity (*NBI*) along a short section in the chirp trajectory Guadalupe River with the water depth shown on the y-axis. The backscatter intensity is expressed as normalized backscatter intensity (*NBI*) in %, i.e., normalized by the maximum backscatter intensity recorded.

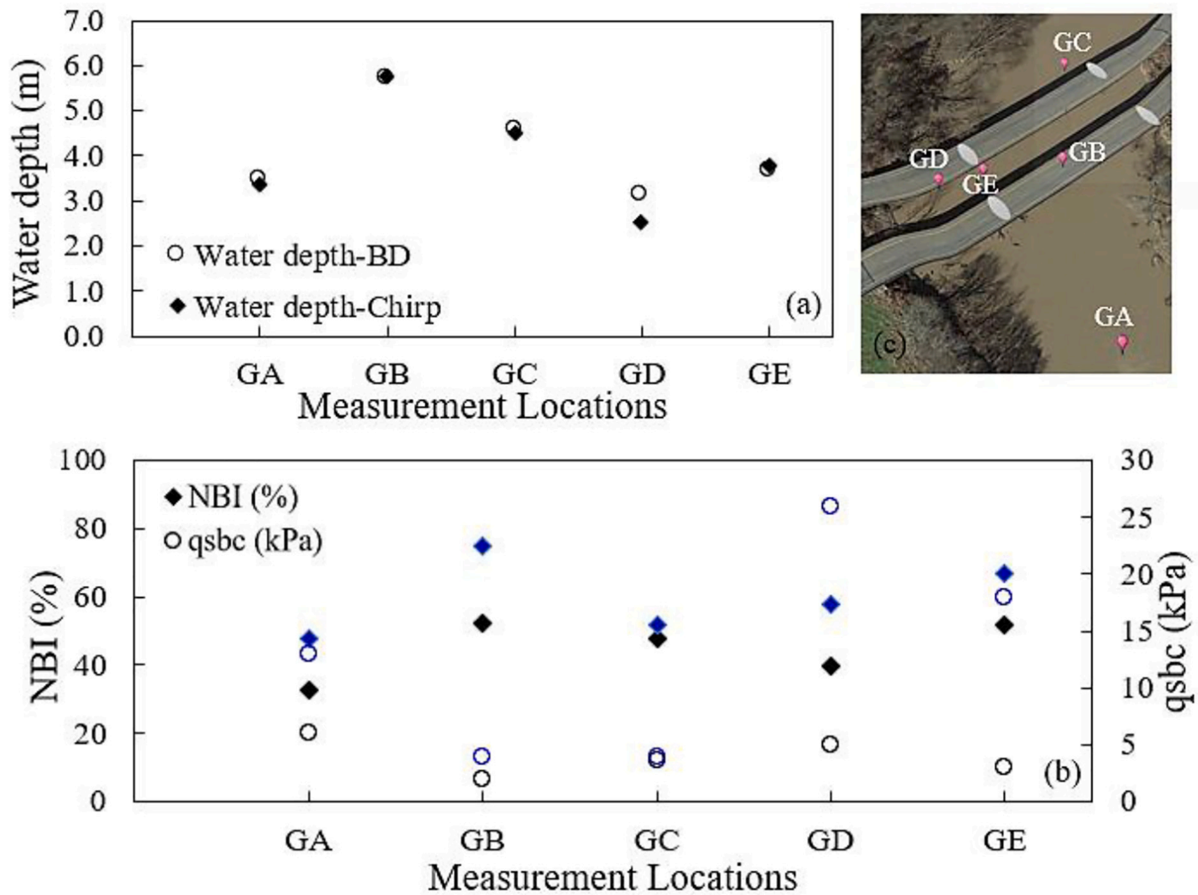

Fig. 5. Results of (a) Water depth, (b) *NBI* and *qsbc* measured from the chirp and PFFP results at different sediment depths: 5–7 cm (black color) and 10–12 cm (blue color) for different locations at the Guadalupe River (c) Chirp measurement location path. (For interpretation of the references to color in this figure legend, the reader is referred to the web version of this article.)

on an average d_{50} of 0.34 mm from samples collected at Guadalupe River. This comes in agreement with the critical velocity estimated by the EFA results (Fig. 6b) that show a V_c of 0.24 m/s is capable of initiating erosion at a rate of 0.1 mm/h for the same location. The average velocity measured during the survey period and the critical velocity calculated are almost equal, indicating that sediment transport is likely for any flow velocities faster than those measured during calm and non-flooding conditions.

4.2. Brazos River

A total of 33 deployments were distributed along two transects at the Brazos River. Transect 1 is orientated across the river, while transect 2 represents a short section along the western riverbank (Fig. S2). Jaber et al. (2020) discuss in more details the variations between the two transects in terms of deceleration profiles, *qsbc*, recorded impact velocities, and grain sizes. PFFP results revealed significant variations

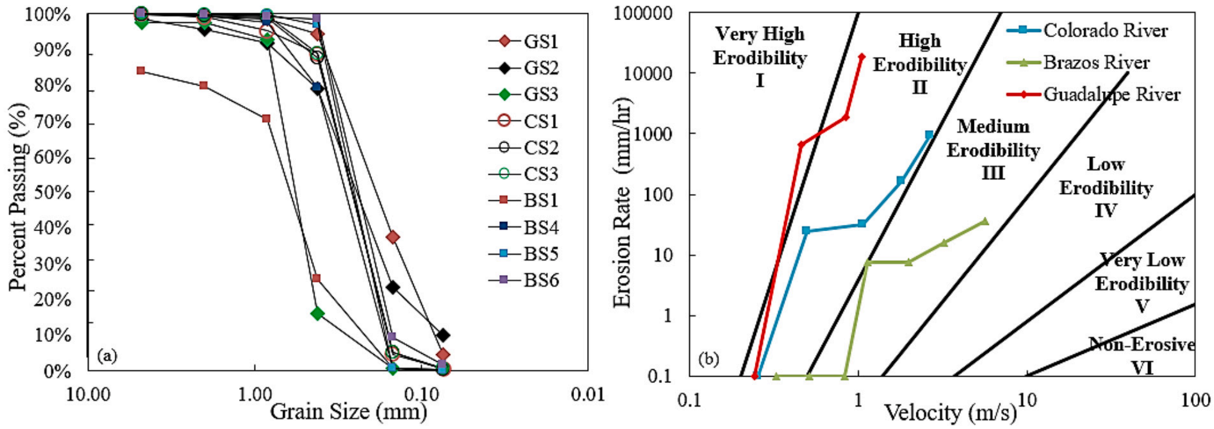

Fig. 6. (a) Gradation curves for samples extracted from the Guadalupe, Brazos, and Colorado riverbanks(1–3) and across the river (4–6) (BS2 and BS3 were omitted). (b) Erosion Function Apparatus (EFA) test results for the Guadalupe River (red), the Colorado River (blue), and the Brazos River (green) in terms of applied flow velocity versus measured erosion rate. (For interpretation of the references to color in this figure legend, the reader is referred to the web version of this article.)

between sediments across the river (Figs. 7, S6). Sediments along the western riverbank (transect 2) exhibit similar behavior: lower *qsbc* values (<25 kPa) and higher penetration depths (Fig. 7) and are associated with finer d_{50} particles (silty sand and fine sand) (Fig. 6a) and predominantly Type A pore pressure responses (Fig. S5). However, profiles of transect 1 record a significantly higher *qsbc* (~200 kPa) at shallower penetration depths and samples obtained showed larger mean grain sizes. Transect 1 profiles can be grouped into two slightly different behaviors, one group with lower *qsbc* values (up to 75 kPa) and deeper penetrations (up to 7 cm), and the other with higher *qsbc* values and shallower penetration depths (up to 4 cm). Type B pressure responses were observed at the end of the transect near the western edge of the riverbank.

The *NBI* measurements at the Brazos River are plotted against the maximum *qsbc* values at a depth between 3 and 5 cm (Fig. S6a). This distance between these measurement points is smaller than the chirp sonars vertical resolution. However, differences are expected based on small-scale topography changes and possible changes in surficial properties. The *NBI* and *qsbc* trends matched from the river center towards the eastern riverbank, which can be considered predominantly sandy. However, a significant mismatch is obvious towards the western riverbank. This may be related to the construction of a temporary boat ramp composed of fine silty sediments, which created soft (low *qsbc*) but a rough surface morphology. The latter may have increased the *NBI*, which was likely further exacerbated by shallow water conditions. This issue led to full saturation of the backscatter signal, masking further interpretation of soil properties. Jaber et al. (2020) provided further comments on the signal saturation in this survey. Water depths from chirp sonar agree mostly with those estimated from PFFP, with few exceptions of shallower water depth recorded by the chirp towards the eastern riverbank (Fig. S6b).

Sediments from the riverbanks seem to be of medium erodibility with the flow velocity required to initiate erosion ~0.33 m/s (Fig. 6b), which is slightly larger than V_c of 0.2 m/s calculated using Eq. 1 for d_{50} of 0.3 mm. Despite the lack of flow velocity estimates from ADCP measurements during the survey period, discharge rates recorded from the closest gage show an estimate of flow velocity ~0.16 m/s, slightly lower than the critical velocity to initiate erosion. Nevertheless, higher flow velocities (up to 0.4 m/s) were observed earlier in July (before survey date), confirming sediment transport processes taking place just before the survey period.

4.3. Colorado River

A total of 49 PFFP deployments were conducted along 5 transects in the Colorado River (Fig. 2). Fig. 9 shows the variations in the maximum *qsbc* and *NBI* results with water depths along different transects. Maximum penetration depths of the PFFP ranged between 4 and 120 cm

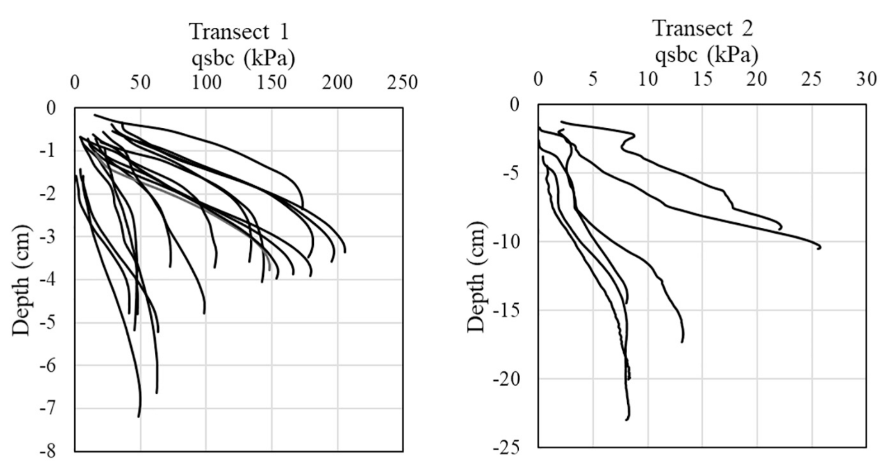

Fig. 7. Quasi-static bearing capacity (*qsbc*) profiles at each transect at Brazos River.

with maximum *qsbc* ranging from under 10 kPa to over 100 kPa, displaying the significant riverbed variability in strength in a relatively small survey area (Fig. 8). The water depths reported for the Colorado River showed an approximate average water depth ~7 m with some geospatial variations on the order of up to 3 m and differences between the PFFP and chirp measurements at few locations along transects 1 and 3 and the entirety of transect 2. The mismatches in water depth between the PFFP and the chirp sonar are likely due to spatial variation in the measurement location of each of the instruments. The ease of the PFFP deployment and lesser concern about hitting any debris facilitated closer drops than the chirp around the piers, as is the case for transects 1 and 3. Therefore, deeper water depths recorded by the PFFP may suggest scour holes in closest proximity to the pier foundations.

The sediments along transect 1 (around the west south bridge pile) had a maximum *qsbc* of 44 kPa with an outlier value of 86 kPa at sediment depth between 12 and 16 cm mainly. The variation in the *NBI* matched the variation in the *qsbc* values with the highest *NBI* of 86% recorded close to 86 kPa (Fig. 9). Transect 2 exhibited stiff soils at both upstream and downstream sides (*qsbc* of 305 and 77 kPa, respectively) with weaker soils in between. The *NBI* values followed the same trend with values up to 80% on the sides. The sediments of transect 3 (around the second upstream pile) displayed more variations in strength which were also reflected by the trends in chirp measurements; however, it should also be noted that the highest *NBI* values represented a saturation of the signal (Fig. 9). The sediments around transect 4 (the bottom pier) were more consistent, as strength did not exceed 50 kPa. The trend of *NBI* variations around the pier matched well with the *qsbc* variations. The *qsbc* values ranged between 18 and 57 kPa along transect 5 with the highest *qsbc*'s detected closer to the eastern riverbank between the two upstream piles at the west side. The eastern side showed high *NBI* values with some noise in the signal.

PWP response type C (Fig. S5) was mostly observed at the Colorado River, specifically at the upstream deployments across the river. Such behavior has been previously associated with coarse sandy sediments (Lucking et al., 2017). Grain size analysis shows that sediments along the riverbanks of the Colorado River are poorly graded fine sands (SP) with less than 1% fines and a constant d_{50} value of 0.27 mm (Fig. 6a). Although the samples collected provide limited insight on the sediment's distribution across the riverbed, the observations suggest that the investigated section of Colorado River sediments was predominantly sandy soils, as is reported by McGowen et al. (1979), where coarser sediment are likely present at the center of the river and finer/muddier sediments exist more towards the riverbank.

The sediments in the Colorado River are classified as highly erodible to very highly erodible based on the EFA test (Fig. 6b). Sediment dynamics were likely not occurring during the survey period due to the low flow velocity of 0.014 m/s recorded by the ADCP. This flow velocity was below the threshold V_c of 0.19 m/s and 0.25 m/s to initiate any sediment motion as was calculated using Eq. 6 and concluded from EFA results (Fig. 6b), respectively. However, the critical flow velocities are easily exceeded when approaching flood conditions.

5. Discussion

5.1. Data collection and quality

Various challenges were encountered with regards to the data collection: (1) All instruments were mounted on or deployed from small

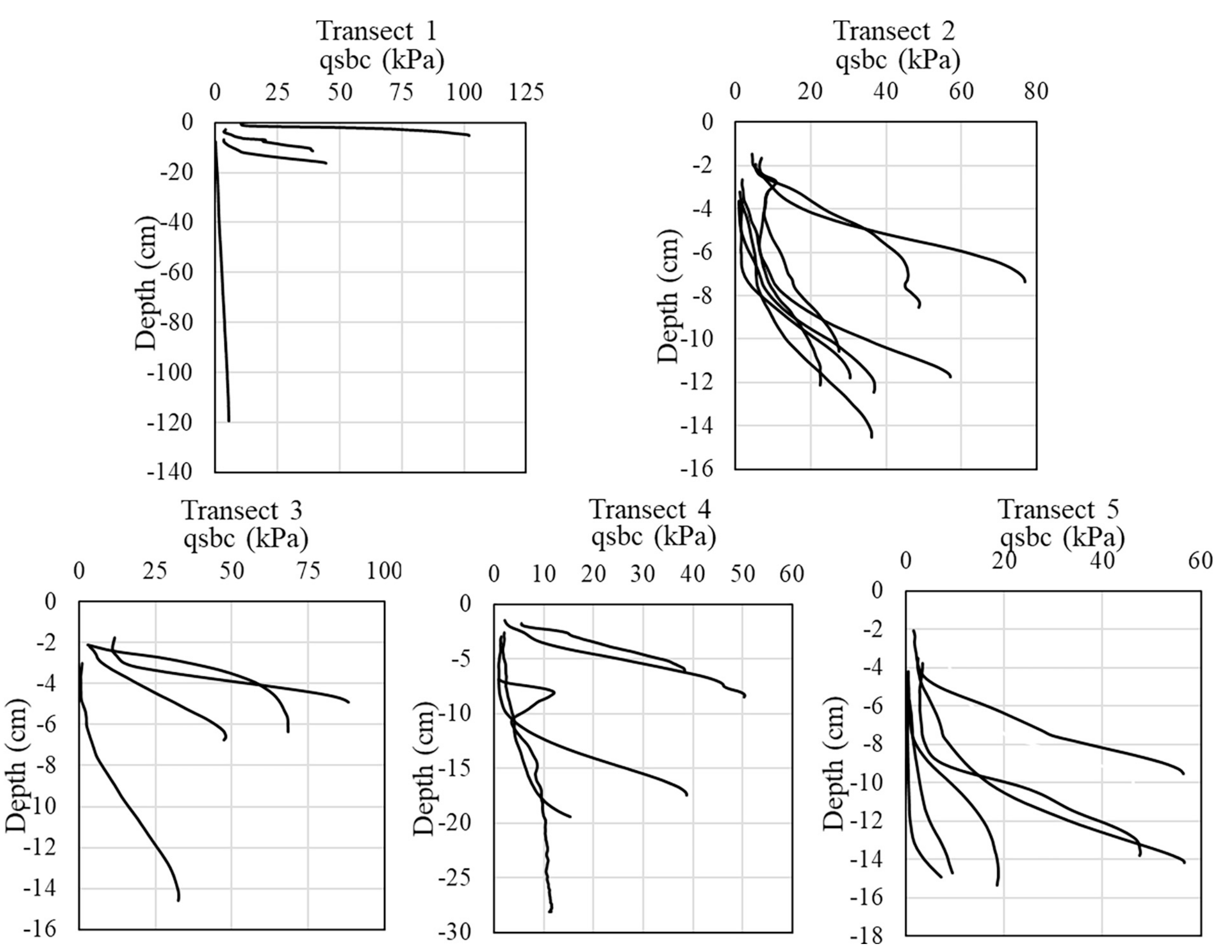

Fig. 8. Quasi-static bearing capacity (*qsbc)* profiles at each transect at Colorado River.

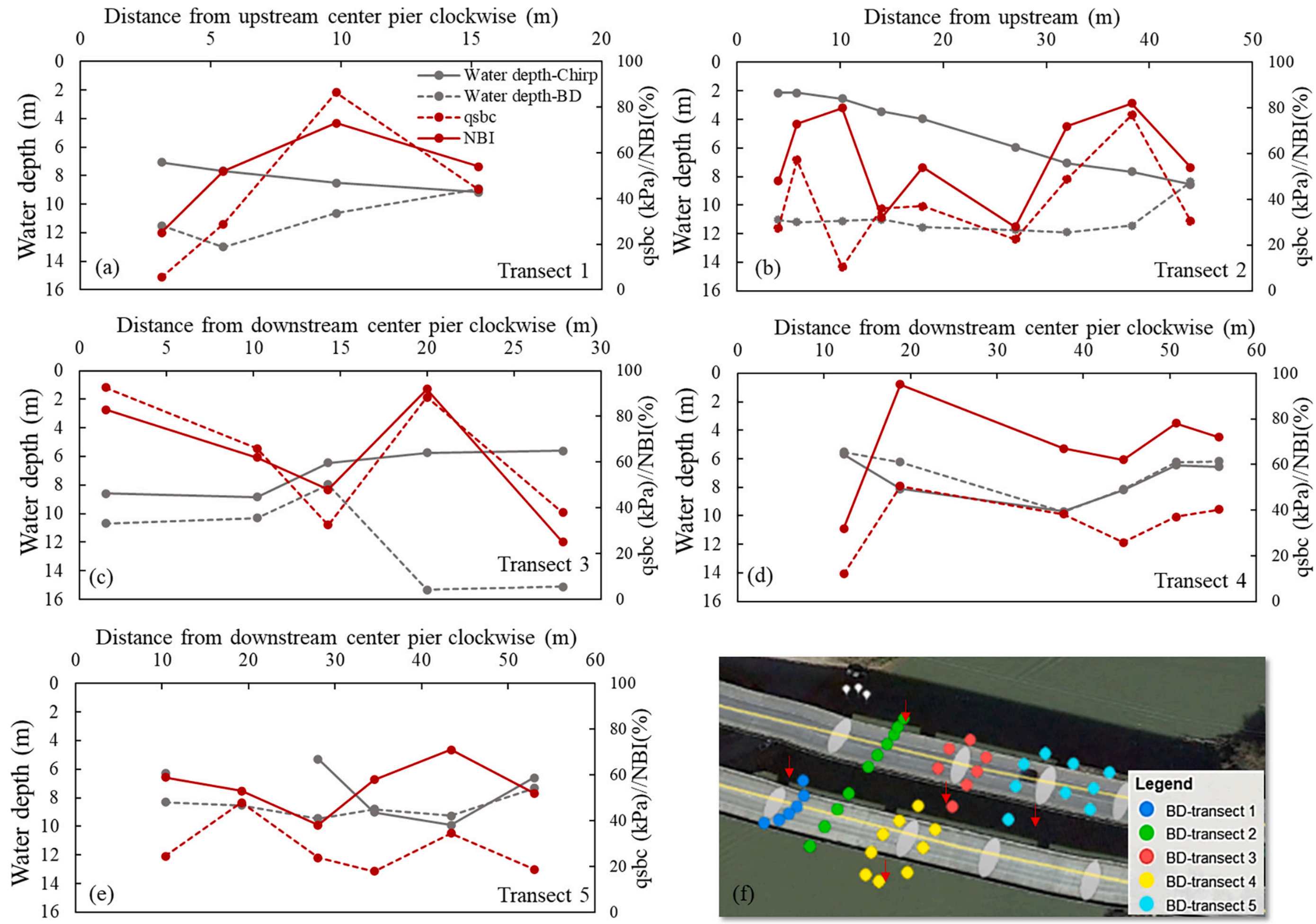

Fig. 9. PFFP and chirp results observed at Colorado River of (a) transect 1 at depth 12–16, (b) transect 2 at depth 10–12 cm, (c) transect 3 at depth 4–6 cm, (d) transect 4 at depth 12–14 cm, (e) transect 5 at depth 5–7 and 15–17 cm and (f) transect locations around bridge piers. Red arrow shows the reference point of each transect. (For interpretation of the references to color in this figure legend, the reader is referred to the web version of this article.)

vessels (canoes and a 2.5 m zodiac) in response to restricted access to the sites and areas of shallow water. (2) Localized changes in hydrodynamic conditions as well as the presence of debris (still from Hurricane Harvey) limited the navigability of the small vessels which affected in incidences data volumes but more often the geospatial match in deployment locations between different devices. With regards to the former, 22% of PFFP deployments were discarded from data processing due to impacts with debris. Furthermore, 65% of the pore pressure recordings from the PFFP were omitted from the analysis, 10% due to lack of pressure rings saturation resulting in a delayed pore pressure response and the others due to an insufficient penetration depth. Challenges associated with maintaining saturation of pore pressure filters and inlets have been previously reported for free fall penetrometer (Seifert et al., 2008). The difficulties can be exacerbated when using small vessels, during high air temperatures, and with limited supporting infrastructure at the sites. Future work should consider innovative solutions to maintain full saturation of pore pressure rings and inlets despite challenging conditions. Despite this number of rejected data sets, the ease of PFFP deployments enabled the collection of a sufficient amount of data to document significant variations in local sediment strength at each investigated river section and between the rivers, as well as with regards to the local geomorphology and presence of infrastructure.

The chirp sonar was easily installed and operated from the small vessels, which needs to be highlighted as such systems are usually deployed at greater water depths and with more sophisticated support vessels. However, the localized presence of debris was mostly unknown (unless it pierced the water surface) due to murky waters and the resulting risk of running the sonar head into debris required slow approaches and often intentional or unintentional deviation from the initially planned transects. The latter was exacerbated by navigational limitations of the small vessels and the use of a handheld GPS with a maximum resolution of 3–5 m in the survey areas. This led to spatial mismatches between the PFFP, and chirp transect lines. It is expected that the deviations in estimated water depths from PFFP and chirp sonar at the Colorado River are resulting from this issue (Fig. 9). Due to scour and debris at the piles of the bridge at the Colorado River, small differences in the measurement location could likely lead to deviations in water depth on the order of a meter or more.

Chirp sonar deployments in water depths ≤5 m are rare. Platt (2018) utilized chirp sonar to investigate the thickness of sand layers in sections of the Colorado River in Grand Canyon, but the investigated areas featured water depths >5 m. The manufacturer of the chirp sonar used in this study suggests a minimum water depth of 1.5 m. The entire Brazos River section investigated is close to this minimum requirement, as well as multiple locations along the other two rivers. It is expected that full saturation of the chirp sonar echo in many locations is related to this issue (particularly where *NBI* >90%). This may have been further exacerbated at the western bank of the Brazos River section, where fine sediments were recently deposited from the building of the boat ramp, and thus, water depths were shallow and surface roughness was high. This led to high *NBI*, while the sediments were actually soft (low *qsbc*). Despite these challenges, similar trends were observed between *NBI* and *qsbc* along the Colorado River transects. Opposing trends were observed at the uppermost surface measurements in the Guadalupe. It is postulated that combined effects of variations in small-scale topography as well as fines contents may lead to complex acoustic returns from these surface sediments.

No direct correlations between the PFFP and the chirp sonar could be established from this study. However, both instruments were deployable from the small vessels and delivered relevant data. Both instruments enabled the determination of local water depth what may be a key information used to refine geospatial matching of results in future studies. Sediment strength determined from the PFFP and normalized backscatter intensity from the chirp sonar agreed well in trend when the measuring locations matched and when surficial seabed sediments were sandy with little fines content. The sites exhibited significant spatial variability in bathymetry and sediment properties. Therefore, navigation would need to be improved to achieve more reliable matching deployment locations. Variations in fines contents as well as small-scale topography (i.e., surface roughness) that can be expected to be related to sediment type as well as location within the river seem to complicate a direct correlation between the chirp response and the PFFP measurements. While this may enable novel strategies of data fusion for a joint interpretation of both instruments for sediment characterization in areas that are difficult to sample and measure with other methods, this will require more research regarding the relationships between geotechnical and geoacoustic properties of different sediment types, surface conditions, and acoustic signals.

5.2. Relevance for local geomorphodynamics post Hurricane Harvey

The investigated section of the Guadalupe River is characterized by significant river meandering and the presence of a bridge spanning across the meandering section of the river. Anthropogenic influences are mostly limited to the wastewater plant efflux pipe upstream of the bridge and local kayakers. Sediment strength measurements of the river surface sediments (penetration depth <0.5 m) suggested a combination of soft to moderately stiff surface sediment upstream of the bridge (Figs. 3 and S4). Five deployments in this area were insufficient to relate the differences to local geomorphological conditions. Downstream of the bridge, surficial sediments were consistently moderately soft with a very soft surface layer of approximately 6–12 cm in thickness over a stiffer substratum, possibly suggesting temporary deposition of sediments mobilized within the meander and deposited downstream of the meander. Current measured velocities in this area were below estimated critical flow velocities needed for sediment transport, supporting this hypothesis. Sediments were soft west of the northern most bridge pile (transect 2) which could be explained by being located in the lee of this bridge pile where sediment deposition from scour may occur. The angle of flow attack on this elongated bridge pile is exacerbated by the river meander and may contribute to a large deposition zone. The results and deployment locations in the vicinity of the western bridge piles appear more complex but seem to suggest stiff sediments upstream of the piles, possibly related to eroded stiff surface sediments and/or debris in possible scour areas. Sediments were again significantly softer in the lee (downstream) of the piles. Scour holes could not be confirmed due to challenges in navigation and chirp measurements with the complex flow patterns and debris around the piles, but the above described suggestions match general expectations of scour and observations of debris. Based on the flow measurements and estimates of critical flow velocity from EFA testing, significant scour appears likely during flood events and may be maintained during moderate flow conditions. Differences in the presence of fines content may complicate such a simplified assessment.

The investigated short section of the Brazos River was affected by major riverbank erosion and slope failures during Hurricane Harvey and recent deposition of finer riverbank sediments at the western riverbank transect. The section experiences little boat traffic due to no nearby access points and steep riverbanks. Surface sediments were hard and sandy in the center of the river section, suggesting little deposition in the river center. Although flow velocities during the survey period were less than critical velocity, flow velocities exceeded V_c a few days before the survey took place and do so regularly. The fresh sediment deposition along the western riverbank is likely similar to the observations that could be made after riverbank slope failures during flood events, creating short-termed shoaling near the shoreline by finer and soft sediments with significant surface roughness. The combined approach of chirp sonar and PFFP highlighted those differences and enabled continuous data collection along the transects.

The investigated section of the Colorado River is characterized by the presence of a major bridge and a small-vessel boat ramp. Boating was actively going on during the survey. Debris was still visibly present at the bridge piles. Damage to a pump station was still unrepaired at the time of the survey. Shortly after Hurricane Harvey, Stark et al. (2017) documented active riverbank failures in the vicinity of the survey location, deposition of up to 30 cm thick sediment layers on the boat ramp and riverbanks, as well as suggested scour at the bridge piles. During the survey presented here (9 months after Hurricane Harvey), scour holes could still be documented. In line with the scour holes, hard surface conditions were identified upstream of the bridge piles, looser sediments in the lee of the bridge piles, and medium conditions at the sides of the piles. Interestingly, transect 2 that was located between piles, still suggested an increase of sediment strength parallel to the upstream ends of the piles.

5.3. Relevance to existing studies

Schrottke et al. (2006) used side scan sonar and a parametric sub-bottom profiler and Seifert and Kopf (2012) used a dynamic CPT in German estuaries known for significant sediment dynamics. Both methods successfully tracked mud sediment dynamics with high temporal and spatial variability in the estuarine environments, but combined geotechnical and geophysical methods were not applied in conjunction in those studies. Osler et al. (2006) conducted co-located measurements of free fall penetrometers with chirp sonar and Boomer seismic profiling in a field study in St. Margaret's Bay, Nova Scotia. However, those authors only presented a correlation of the free fall penetrometer results to core samples and bathymetry. Stark et al. (2011) demonstrated the use of combined PFFP, multi-beam echo sounder, and acoustic Doppler current profiler to study dynamics of subaqueous dunes but did not apply acoustic sub-bottom profiling. While the studies mentioned herein represent an important motivation for this study, they did not attempt a direct combined approach of in-situ geotechnical testing and sub-bottom profiling of sites affected by sediment dynamics.

Prins and Andresen (2021) combined geophysical and geotechnical methods using 3D and high-resolution 2D seismic data and cone penetration test (CPT) data. From the combined results, the authors derived geotechnical stratigraphy in the Southern Danish Central Graben in the North Sea. The study also succeeded in identifying the erosional base and channel infill, representing an application of joint geotechnical testing and chirp sonar for the investigation of previous sediment dynamics. However, a direct correlation between seismic facies and CPT response could not be established, hindered mainly by the difference in resolution provided by each measurement. (Prins and Andresen, 2021) and this study both highlight the potential of fusing geotechnical in-situ testing and chirp sonar for the investigation of sediment dynamics. Both studies also agree on the value and difficulty on direct quantitative correlations between the methods. An important difference between this study and Prins and Andresen (2021) is that this article focuses on a high vertical resolution of the surface sediment layers and was performed in shallow waters, both pushing current capabilities regarding the geotechnical and geophysical methods.

6. Conclusion

This paper describes combined geotechnical and geoacoustic measurements of sections of the Guadalupe, Brazos, and Colorado Rivers conducted in 2018 and motivated by the observed impacts during Hurricane Harvey in 2017. The study focuses on investigating the combined use of a portable free fall penetrometer (PFFP) and a chirp sonar for improved site characterization in the context of local geomorphodynamics and riverine environments. Both instruments were found suitable for deployment from small vessels of opportunity (canoes, dinghies, etc.) and unknown riverbed conditions. The variations in sediment strength and water depth measured by the PFFP among the rivers overall agreed with the variations in the backscatter intensities measured by the chirp sonar at sandy sites and sites with limited variations in surface roughness. Mismatches were associated with spatial variations resulting from navigational limitations, as well as likely to transitions in fines contents and surface roughness. Laboratory results and flow velocity measurements suggested that while little or no sediment dynamics were ongoing during the measurements, sediment dynamics are likely to initiate with little increase in flow velocity. Variations in geotechnical and geoacoustic riverbed conditions appeared related to local sediment dynamics and scour during Hurricane Harvey but also to flood conditions between the hurricane event and the survey. Further research establishing a better understanding of the correlations between geotechnical and geoacoustic properties in areas with complex variations in sediment particle size distributions and local geomorphodynamics is needed. Advancements in analyzing combined geotechnical and geoacoustic site investigation will contribute to improve the prediction and assessment of scour, erosion, and sediment dynamics in general after extreme events in riverine areas of difficult access.

Data availability statement

Some or all data, models, or code generated or used during the study are available in a repository or online in accordance with funder data retention policies. (Stark, N. Jafari, N. Ravichandran, R. Jaber, R. (2020) "Combined Geotechnical and Geophysical Investigation of Texas Rivers Post Hurricane Harvey.", in Combined Geotechnical and Geophysical Investigation of Texas Rivers Post Hurricane Harvey. DesignSafe-CI. https://doi.org/10.17603/ds2-835m-zp94. Some or all missing data, models, or code that support the findings of this study are available from the corresponding author upon reasonable request. Supplemental figures, captioned as Fig.S1-Fig.S6, are published in an accompanying Data in Brief article with additional information submitted along with this manuscript.

Declaration of Competing Interest

The authors declare that they have no known competing financial interests or personal relationships that could have appeared to influence the work reported in this paper.

Acknowledgments

The authors would like to acknowledge the National Science Foundation for funding the research and work presented through grant CMMI-1822307. The authors express gratitude to Julie Paprocki, Dennis Kiptoo, Matthew Florence, and Brian Harris for their data collection efforts. The authors would also like to thank Jean-Louis Briaud and Iman Shafii for their assistance with the EFA testing. The authors would also like to thank the reviewers of this article for constructive feedback that contributed to this article.

Appendix A. Supplementary data

Supplementary data to this article can be found online at https://doi.org/10.1016/j.enggeo.2021.106324.

References

Abelev, A., Herdic, P., Vermillion, M., Amon, D., 2017. Geotechnical and geoacoustic investigation of seafloor sediments on boston harbor approaches. In: *Naval Research Laboratory*. (No. NRL/MR/7420-17-9707) Washington, DC.

Akal, T., Stoll, R.D., 1995. An expendable penetrometer for rapid assessment of seafloor parameters. In: Proc., OCEANS'95 MTS/IEEE In "Challenges of Our Changing Global Environment", San Diego, pp. 1822–1826.

Albatal, A., Wadman, H., Stark, N., Bilici, C., McNinch, J., 2019. Investigation of spatial and short-term temporal nearshore sandy sediment strength using a portable free fall penetrometer. J. Coast. Eng. 143, 21–37.

Albatal, A., Stark, N., Castellanos, B., 2020. Estimating in situ relative density and friction angle of nearshore sand from portable free-fall penetrometer tests. Can. Geotech. J. 57 (1), 17–31.

Anderson, J.T., Van Holliday, D., Kloser, R., Reid, D.G., Simard, Y., 2008. Acoustic seabed classification: current practice and future directions. ICES J. Mar. Sci. 65 (6), 1004–1011.

ASTM D2487–-11, 2021. Standard Practice for Classification of Soils for Engineering Purposes (Unified Soil Classification System). *ASTM International*, West Conshohocken, PA.

ASTM D6913–-17, 2021. Standard Test Methods for Particle-Size Distribution (Gradation) of Soils Using Sieve Analysis. *ASTM International*, West Conshohocken, PA.

Blake, E.S., Zelinsky, D.A., 2018. National Hurricane Center Tropical Cyclone Report Hurricane Harvey. National Hurricane Center, National Hurricane Center Tropical Cyclone Report Hurricane Harvey.

Briaud, J.-L., 2013. Geotechnical Engineering Unsaturated and Saturated Soils. Wiley, *Hoboken*, NJ.

Briaud, J.L., Ting, F.C., Chen, H.C., Gudavalli, R., Perugu, S., Wei, G., 1999. SRICOS: Prediction of scour rate in cohesive soils at bridge piers. J. Geotech. Geoenviron. Eng. 25 (4), 237–246.

Briaud, J.-L., Ting, F., Chen, H.C., Cao, Y., Han, S.-W., Kwak, K., 2001. Erosion function apparatus for scour rate predictions. J. Geotech. Geoenviron. Eng. 127 (2), 105–113.

Briaud, J.-L., Hamn-Ching, Chen, Park, Siyoung, 2002. Predicting meander migration: evaluation of some existing techniques. In: Chen, Hamn-Ching, Briaud, Jean-Louis (Eds.), *Proc. of 1st Intl. Conference on Scour of Foundations*, College Station, pp. 1061–1080.

Brown, C.J., Todd, B.J., Kostylev, V.E., Pickrill, R.A., 2011. Image-based classification of multibeam sonar backscatter data for objective surficial sediment mapping of Georges Bank, Canada. Cont. Shelf Res. 31 (2), S110–S119.

Chow, S.H., Airey, D.W., 2013. Soil strength characterisation using free-falling penetrometers. Géotechnique 63 (13), 1131–1143.

Collins, M., Ferentinos, G., Banner, F.T., 1979. The hydrodynamics and sedimentology of a high (tidal and wave) energy embayment (Swansea Bay, northern Bristol Channel). Estuar. Coast. Mar. Sci. 8 (1), 49–74.

Dayal, U., Allen, J.H., 1973. Instrumented impact cone penetrometer. Can. Geotech. J. 10 (3), 397–409.

Dorvinen, J., Stark, N., Hatcher, B., Hatcher, M., Leys, V., Kopf, A., 2018. In Situ assessment of sediment erosion and consolidation state using a free-fall penetrometer: sydney harbour, nova scotia. J. Waterw. Port Coast. Ocean Eng. https://doi.org/10.1061/(ASCE)WW.1943-5460.0000423, 04017041.

EcoEnvironmental, August 1, 2019. Ponar 'Grab' Samplers. http://ecoenvironmental.com.au/sales/soil-sampling/ponar-grab-samplers/.

Gavin, K., Prendergast, J.L., 2018. Reliable performance indicators for bridge scour assessments. In: *Proc. of TU1406 COST Action*, Barcelona.

Harris, M.M., Avera, W.E., Abelev, A., Bentrem, F.W., Bibee, L.D., 2008. Sensing shallow seafloor and sediment properties, recent history. In: *Proc. of Oceans 2008,*MTS/IEEE, Quebec, pp. 1–11.

Holland, C.W., 2002. Coupled scattering and reflection measurements in shallow water. J. Ocean. Eng. 27 (3), 454–470.

Houlsby, G.T., Ruck, B.M., 1998. Interpretations of Signals from an Acoustic Cone Penetrometer, Geotechnical Site Characterization. In: *Proc. ISC-1*, Atlanta, pp. 1075–1080.

Jaber, R., Stark, N., Jafari, N., Ravichandran, N., 2020. In situ geotechnical investigation of a short section of the brazos river post-hurricane harvey using a portable free fall penetrometer. In: Proceedings Geo-Congres, ASCE, Minnesota, pp. 760–768.

Jackson, D.R., Richardson, M.D., 2007. High-frequency seafloor acoustics, The Underwater Acoustics Series. Springer, New York.

Link, O., García, M., Pizarro, A., Alcayaga, H., Palma, S., 2020. Local scour and sediment deposition at bridge piers during floods. J. Hydraul. Eng. 146 (3), 04020003.

Long, M., Trafford, A., McGrath, T., O'Connor, P., 2020. Multichannel analysis of surface waves (MASW) for offshore geotechnical investigations. Eng. Geol. 272, 105,649.

Lucking, G., Stark, N., Lippmann, T., Smyth, S., 2017. Variability of in situ sediment strength and pore pressure behavior of tidal estuary surface sediments. Geo-Mar. Lett. 37 (5), 441–456.

Mayne, P.W., 2014. Interpretation of geotechnical parameters from seismic piezocone tests. In: *Proc. of 3rd International Symposium on Cone Penetration Testing*, Las Vegas, pp. 47–73.

McGowen, J.H., Byrne, J.R., Wilkinson, B.H., 1979. Geochemistry of bottom sediments–Matagorda Bay system, Texas. Austin. University of Texas at Austin, Bureau of Economic Geology.
Mcneill, R., 1979. Enhancement of geophysical soil profiles using instrumented marine sediment penetrators. In: Proc. of *Offshore Technology Conference. Houston*.
Mosher, D.C., Christian, H., Cunningham, D., MacKillop, K., Furlong, A., Jarrett, K., 2007. The harpoon free fall cone penetrometer for rapid offshore geotechnical assessment. In: Proc. of *6th International Conference on Offshore Site Investigation and Geotechnic, Society for Underwater Technologies*, London.
Mumtaz, M.B., Stark, N., Brizzolara, S., 2018. Pore pressure measurements using a portable free fall penetrometer. In: *Proc. 4th International Symposium on CPT*, Delft/461.
Neto, A.A., Mendes, J.D.N.T., Souza, J.M.G.D., Redusino, M., Pontes, R.L.B., 2013. Geotechnical influence on the acoustic properties of marine sediments of the santos basin, brazil. Mar. Georesour. Geotechnol. 31 (2), 125–136.
NWIS (National Water Information System), 2019. USGS Current Conditions for the Nation-Station 08114000. https://nwis.waterdata.usgs.gov/nwis/uv? (June 10, 2019).
Osler, J.C., Hines, P.C., Trevorrow, M.V., 2002. Acoustic and in-situ techniques for measuring the spatial variability of seabed geoacoustic parameters in littoral environments. In: Pace, N.G., Jensen, F.B. (Eds.), Impact of Littoral Environmental Variability of Acoustic Predictions and Sonar Performance. Springer, Dordrecht, pp. 83–90.
Osler, J., Furlong, A., Christian, H., Lamplugh, M., 2006. The integration of the free fall cone penetrometer (FFCPT) with the moving vessel profiler (MVP) for the rapid assessment of seabed characteristics. The International hydrographic review.
Platt, A.S., 2018. Estimating Riverbed Sand Thickness Using CHIRP Sonar: Case Study from the Colorado River in Grand Canyon. Master dissertation. Northern Arizona University.
Preston, J., Collins, W., Mosher, D., Poeckert, R., Kuwahara, R., 1999. The strength of correlations between geotechnical variables and acoustic classifications. In: Proc., Oceans 99. MTS/IEEE, Seattle, pp. 1123–1128.
Prins, L.T., Andresen, K.J., 2021. A geotechnical stratigraphy for the shallow subsurface in the Southern Central Graben, North Sea. Eng. Geol. 286, 106,089.
Qin, R., Khakzad, N., Zhu, J., 2020. An overview of the impact of Hurricane Harvey on chemical and process facilities in Texas. Int. J. Dis. Risk Reduct. 45, 101,453.
Randolph, M.F., 2016. New tools and directions in offshore site investigation. Aust. Geomech. 51 (4), 81–92.
Saleh, M., Rabah, M., 2016. Seabed sub-bottom sediment classification using parametric sub-bottom profiler. NRIAG J. Astron. Geophys. 5 (1), 87–95.
Sandven, R., 2010. Influence of test equipment and procedures on obtained accuracy in CPTU. In: *Proc. of 2nd International Symposium on Cone Penetration Testing*, (CPT'10), CA.
Schrottke, K., Becker, M., Bartholomä, A., Flemming, B.W., Hebbeln, D., 2006. Fluid mud dynamics in the Weser estuary turbidity zone tracked by high-resolution side-scan sonar and parametric sub-bottom profiler. Geo-Mar. Lett. 26 (3), 185–198.
Seifert, A., Kopf, A., 2012. Modified dynamic CPTU penetrometer for fluid mud detection. J. Geotech. Geoenviron. 138 (2), 203–206.
Seifert, A., Stegmann, S., Mörz, T., Lange, M., Wever, T., Kopf, A., 2008. In situ pore-pressure evolution during dynamic CPT measurements in soft sediments of the western Baltic Sea. Geo-Mar. Lett. 28 (4), 213.
Shidlovskaya, A., Briaud, J.-L., Chedid, M., Keshavarz, M., 2016. Erodibility of soil above the groundwater level: some test results. In: Proc., of 3rd European Conference on Unsaturated Soils, Paris, p. *624*.
Shields, A., 1936. Application of Similarity Principles and Turbulence Research to Bed-Load Movement. Hydrodynamics Laboratory, *California Institute of Technology*, p. 167.
Silva, M.F., White, D.J., Bolton, M.D., 2006. An analytical study of the effect of penetration rate on piezocone tests in clay. Int. J. Numer. Anal. Methods Geomech. 30 (6), 501–527.
Spooner, I.S., Williams, P., Martin, K., 2004. Construction and use of an inexpensive, lightweight free-fall penetrometer: applications to paleolimnological research. J. Paleolimnol. 32 (3), 305–310.
Stark, N., Kopf, A., 2011. Detection and quantification of sediment remobilization processes using a dynamic penetrometer. In: Proc. of *Oceans 2011,* IEEE/MTS, Waikoloa.
Stark, N., Hanff, H., Svenson, C., Ernstsen, V.B., Lefebvre, A., Winter, C., Kopf, A., 2011. Coupled penetrometer, MBES and ADCP assessments of tidal variations in surface sediment layer characteristics along active subaqueous dunes, Danish Wadden Sea. Geo-Mar. Lett. 31 (4), 249–258.
Stark, N., Jafari, N., Ravichandran, R., Shafi, I., Smallegan, S., Bassal, P., Figlus, J., 2017. The geotechnical aspects of coastal impacts during hurricanes harvey. In: GEER Association Report No GEER-054. Version 1.
Stoll, R.D., Akal, T., 1999. XBP - tool for rapid assessment of seabed sediment properties. Seal. Technol. 40 (2), 47–51.
Stone, G.W., Liu, B., Pepper, D.A., Wang, P., 2004. The importance of extratropical and tropical cyclones on the short-term evolution of barrier islands along the northern Gulf of Mexico, USA. Mar. Geol. 210 (1–4), 63–78.
SyQwest, 2016. StrataBox HD Chirp Operations and Maintenance Manual. http://www.syqwestinc.com/products/sub-bottom-profilers/stratabox (June 5, 2019).
Wang, J., Stewart, R., 2015. Inferring marine sediment type using chirp sonar data: Atlantis field, Gulf of Mexico. Soc. Explorat. Geophys. 2385–2390.
Xu, F., Tao, J., Zhou, Z., Coco, G., Zhang, C., 2016. Mechanisms underlying the regional morphological differences between the northern and southern radial sand ridges along the Jiangsu Coast, China. Mar. Geol. 371, 1–17.
Zane, D.F., Bayleyegn, T.M., Hellsten, J., Beal, R., Beasley, C., Haywood, T., Wolkin, Wiltz-Beckham D., A. F., 2011. Tracking deaths related to Hurricane Ike, Texas, 2008. Dis. Med. Public Health Preparedness 5 (1), 23–28.